

Screening and preliminary analysis of differentially expressed genes in quail embryos for feather colour based on RNA-Sequencing

Y.Q. Hu¹, X.H. Zhang^{1,2#}, Y.Z. Pang^{1,2}, Y.X. Qi^{1,2}, Q.K. Wang¹, Y.W. Zhao¹, Z.W. Yuan¹, T. Wang¹, L.K. Huo¹ & S.W. Ren¹

¹ College of Animal Science, Henan University of Science and Technology, Luoyang, Henan 471003, China

² Luoyang Key Laboratory of Animal Genetics and Breeding, Luoyang, Henan 471003, China

(Submitted 19 March 2022; Accepted 23 January 2023; Published 10 July 2023)

Copyright resides with the authors in terms of the Creative Commons Attribution 4.0 South African Licence.

See: <http://creativecommons.org/licenses/by/4.0/za>

Condition of use: The user may copy, distribute, transmit and adapt the work, but must recognise the authors and the South African Journal of Animal Science.

Abstract

The purpose of this study was to use RNA-Sequencing (RNA-Seq) to screen differentially expressed genes (DEGs) and analyse transcriptomic data from embryonic skin tissues of maroon-feather and white-feather quails. The transcriptome of embryonic skin tissues from quails was sequenced using the Illumina HiSeq™ 2000 sequencing platform. A total of 2 512 DEGs were found. Of these, 550 DEGs were up-regulated and 1 562 DEGs were down-regulated in the skin tissues of white-feather quail embryos. Five hundred and ninety-seven DEGs were enriched and annotated into 50 entries in Gene Ontology (GO) database. The total number of DEGs annotated in each entry in the Kyoto Encyclopedia of Genes and Genomes (KEGG) database was 341, enriched in 230 pathways, of which the tight junction pathway and neuroactive ligand-receptor interaction were the most significantly enriched. Candidate genes were analysed using real-time quantitative reverse transcription polymerase chain reaction (to verify the accuracy and reliability of the RNA-Seq results). The relative expression of agouti signalling protein (*ASIP*) and DOPA decarboxylase (*DDC*) in white-feather quails were increased. Relative expression of homeobox D1 (*HOXD1*), cathepsin D (*CTSD*), keratin 2 (*KRT2*), methyl-CpG binding domain protein 2 (*MBD2*), and melatonin receptor 1 (*MT1*) were decreased. The results of this study provide useful data on the analysis of the feather colour regulatory mechanism in white- and maroon-feather quails.

Keywords: gene expression; GO; KEGG; pigment; qRT-PCR; RNA-Seq

Corresponding author: zhangxiaohui78@126.com

Introduction

In quail, as in most birds, the variability of plumage colour comes from the diversity of pigments, the pattern of pigment deposition in different parts of the feathers, and the modular organization of feather bundles throughout the bird's body (Abolins-Abols *et al.*, 2018). The most obvious phenotypic difference between maroon-feather and white-feather quails comes from the colour of their feathers, which is mainly determined by melanin, carotenoid pigments, and porphyrin pigments (Inaba *et al.*, 2020). Birds with melanin will have black, brown, and grey feathers; birds with carotenoids will have red, yellow, orange, and purple feathers; and porphyrin pigments will have pink, green, and other colours (Javůrková *et al.*, 2019). Structural colouration is an optical effect resulting from changes in the direction of light transmission caused by certain specific microstructural arrangements, the most typical example being the green-headed feature of male mallards. Birds also have a great diversity of plumage, especially in domesticated birds, where feathers play a role in heat retention, mate attraction, communication, camouflage, and skin protection (Ng *et al.*, 2018).

Although plumage colour traits of quail have been widely used in the production of quail (e.g., Beijing white-feather and Korean maroon-feather quail) for eggs (Wang *et al.*, 2022), the genetics responsible for such plumage colour differences have not been adequately studied. Studies of variation in plumage colour phenotypes generally focus on genes associated with pigment synthesis. The content and distribution of melanin is the most important factor in phenotypic colour differences, since almost

all organisms can synthesize melanin on their own. The pigment in maroon-feather quail feathers is mainly melanin, and the content and distribution of melanin is the main reason for the dark and light patterns of maroon-feather quail (Javůrková *et al.*, 2019). It has been shown that the black and brown coating pattern of embryos is altered when the pigmentation pattern of Japanese quail is abnormal, and the distribution pattern of mutants expressing the Mel EM antigen or true melanogenic enzyme mRNA (*DCT*, *TYRP1*) in feather buds and epidermis is greatly disturbed, resulting in systemic haemorrhagic death in most embryos (Niwa *et al.*, 2003). The melanin deposition process is complex and divided into three main stages: melanocyte development, pigment production, and pigment distribution. True melanin is synthesized and transported to keratinocytes closer to the skin surface, and mature melanin vesicles containing melanin are transferred to adjacent keratin-forming cells through the tip of melanocyte dendrites (Sun *et al.*, 2020). White-feathered quail are mutants of wild-type quails with low pigment content in their feathers. The reasons for this difference are inextricably related to the mechanism of synthesis and transport of melanin by individual quail. The difference between maroon-feather and white-feather quail plumage colour arises from the differential expression of genes related to the plumage colour trait; the high expression of genes favouring melanin synthesis inevitably leads to a deeper colouration of the relevant tissues in the corresponding species, while the opposite occurs in the albino (Tsudzuki *et al.*, 1992).

To investigate the genetic mechanism of plumage colour differences, this study identified differentially expressed genes (DEGs) in embryonic skin tissues of white- and maroon-feather quail using RNA-Sequencing (RNA-Seq), analysed the biological functions and signalling pathways of DEGs, and explored the interaction patterns of DEGs to elucidate the molecular mechanism of plumage colour differences between white- and maroon-feather quails, and then screened the important genes and pathways associated with plumage colour.

Materials and Methods

All experimental procedures involving quail followed the policies and guidelines of the Henan University of Science and Technology Animal Welfare and Use Committee (Ethics Code: DKY2020102018).

A total of 32 fertilized eggs of purebred white- and maroon-feather quails were selected from the experimental farm of Henan University of Science and Technology. All the fertilized eggs were acclimated under standard laboratory conditions (ventilated room, 38 ± 0.5 °C, 60 ± 5 % humidity, 12 hours light/dark cycle). Embryonic skin tissues of white- and maroon-feather quail were sampled at 8, 10, 12, and 14 days, respectively, with four replicates at each stage. Total RNA was extracted from each embryonic skin tissue sample (0.2 g) using RNAiso Plus (Solarbio, China), according to the manufacturer's procedure. Total RNA quality and quantity were measured using 1% (w/v) agarose gel electrophoresis and a NanoDrop D2000 (Thermo Fisher Scientific, USA). The qualified total RNA (RIN >7) was reverse transcribed to cDNA using a kit (TSK 302, Beijing TsingKe Biotech Co., Ltd, China). Three samples of 10-d quail embryo skin tissues were taken from the samples and sent to Berry Hutchinson corporation in dry ice for RNA-Seq.

The raw reads were obtained using high-throughput sequencing (Illumina platform, HiSeq™ 2000). The clean reads were obtained by removing the reads containing adaptors (FastQC). The clean reads were obtained by removing the reads with a proportion of N greater than 10% using the FastQC tool. It also removed low-quality reads (the reads that have nucleobase Q value ≤ 5 and a proportion of > 50% of the whole read) using FastQC. The sequenced reads were spliced and assembled using Trinity software (version: V2 014-07-17; the parameters were the default parameters) for transcriptome splicing. The clean reads of each sample were compared to the reference sequence (GCA_001577835.2) using Bowtie (V1.0.0) software. The number, length, and GC content of the assembled unigenes were counted. The unigene sequences were aligned with Gene Ontology (GO), Kyoto Encyclopedia of Genes and Genomes (KEGG), euKaryotic Ortholog Groups (KOG), NCBI non-redundant protein sequences (NR), NCBI nucleotide sequences (NT), and Swiss-Prot databases through BLASTx (BLAST parameter, E-value $\leq 1 \times 10^{-5}$ and HMMER parameter, E-value $\leq 1 \times 10^{-10}$), to finally obtain the annotation information of the unigenes.

The fragments per kilobase of transcript per million mapped reads (FPKM) value was calculated for each unigene per sample's expression quantity using RSEM (v1.2.15) software. The differential expression of unigenes in each sample was analysed using edgeR package in R. The DEGs were obtained according to a false discovery rate (FDR) <0.05 and \log_2 |foldchange| >1.

Using Database for Annotation, Visualization, and Integrated Discovery (DAVID) v6.8 software, the DEGs were compared with the GO database to obtain GO functional annotation information of the DEGs. The threshold used for significant enrichment was $P < 0.05$, and the KEGG database was used to compare the DEGs to obtain the pathway annotation information of the significant enrichment of

DEGs.

To verify the accuracy of the sequencing results, the primers in Table 1 were designed to detect the expression of candidate DEGs (Table 4) in white- and maroon-feather quails using qPCR. The internal reference gene was *GAPDH*. Primer 5.0 was used to design primers for the candidate genes, and the primers were synthesized at Oakdingsheng (Wuhan) Biotechnology Co. The relative expression of DEGs was calculated using the $2^{-\Delta\Delta Ct}$ method (Livak & Schmittgen, 2001). SPSS Statistics 17.0 software was used for *t*-test analysis. GraphPad prism 8.0 was used for graphing.

Table 1 The information of template sequences, primer sequences, product length, and annealing temperature of qRT-PCR primers for candidate genes

Gene	Template sequence	Primer sequences (5'→3') ¹	Product length (bp)	Annealing temperature (°C)
ASIP	XM_015881357.2	F: TGCTCTGCTACAGTTTGC R: TTATTCTCTGCCTCTTTTC	172	50
KRT2	XM_015887006.2	F: TGAAGAGGAAATCAACAAAAGG R: TGAAGAGGAAATCAACAAAAGG	196	56.6
CTSD	XM_015863832.2	F: CCTCACCAAGTTCACCTCCAC R: ATGCCAATCTCACCATATAAC	177	59.1
MBD2	XM_015850434.2	F: GAAAATGATGCCGTCCAA R: AAGCCTCTTCTCCAGAACA	229	56.3
DDC	XM_015854339.2	F: TAGGTTGTGTGGCTTCTCTT R: CGTCTGATGGTTTTTGTCTT	205	56.6
MT1	XM_032447116.1	F: AGTAGCAGCCCCACCT R: GCACACCACATGGCAAACA	127	58.6
HOXD1	XM_032445884.1	F: CCTCGTATACCTCCCCTTCTT R: TCTTTGCTGTCATTGCCAC	225	59.1
GAPDH	XM_015873412.2	F: TGCCGTCTGGAGAAACC R: CAGCACCCGCATCAAAG	160	55.7

¹F: forward primer; R: reverse primer

The reaction system for qPCR was 20 μ l (cDNA 1 μ L, upstream and downstream amplification primers 0.75 μ L each, SYBR® Premix Ex Taq™ II (2x) 10 μ L, ddH₂O 7.5 μ L). Reaction conditions: pre-denaturation at 95 °C for 3 min; denaturation at 95 °C for 30 s, annealing for 30 s (set according to the annealing temperature of each primer), extension at 72 °C 20 s, 40 cycles. The signal was collected during the extension phase. The melting curve was increased by 0.5 °C every 5 s from 65 °C to 95 °C.

Results and Discussion

The total amount of RNA in embryonic skin tissue of maroon- and white-feather quails was greater than 10 ng/ μ L (1 500–2 500ng/ μ L), and the integrity (RIN value) was greater than 7, and both 18S:28S were greater than 2.2. The above results indicate that the RNA integrity was good and not degraded, which meets the requirements of database construction and can be used for the subsequent analysis.

Each sample generated 9.7GB of data, including 399 286 896 pairs of reads. Based on the inference of quail genome information (the length of quail genome is 531.96 MB), the data of samples basically met the coverage of 15.6 374 times per sample. After the quality control and reads splicing, a total of 77 228 non-redundant contigs were obtained. The N50 length was 2 204 bp, the average length was 1 153.63 bp, the average GC content of contigs was 45.85%. The percentage of reads (mapped reads and unique mapping reads) to the reference genome (GCA_001577835.2) and the unigenes with annotation information showed that the assembly results could meet the needs of information analysis (Table 2 and Table 3).

Table 2 The statistics of total reads, mapped reads (ratio), unique mapped reads (ratio), and multi mapped reads (ratio) for samples

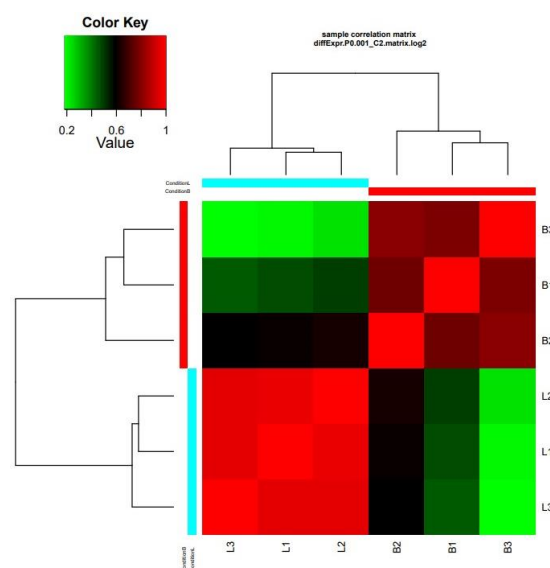
Sample name	Total reads	Mapped reads (ratio)	Unique mapped reads (ratio)	Multi mapped reads (ratio)
B1	57 930 394	42 246 590(72.93%)	29 929 746(70.85%)	12 316 844(29.15%)
B2	42 866 114	30 815 030(71.89%)	21 844 734(70.89%)	8 970 296(29.11%)
B3	1.04E+08	74 834 564(72.18%)	52 583 030(70.27%)	22 251 534(29.73%)
L1	63 329 726	45 175 862(71.33%)	32 436 324(71.80%)	12 739 538(28.20%)
L2	68 441 906	48 796 446(71.30%)	34 893 540(71.51%)	13 902 906(28.49%)
L3	63 041 374	44 844 494(71.14%)	32 305 042(72.04%)	12 539 452(27.96%)

Total Reads: Total number of clean reads after filtering; Mapped reads (ratio): the number of reads of the reference genes on the pair (ratio); Unique mapped reads (ratio): the number of reads on the unique pair (ratio); Multi mapped reads (ratio): the number of reads of multiple loci (ratio)

Table 3 Gene annotation statistics

Functional Database	Annotated Number	300≤ length <1000	Length ≥1000
GO Annotation	17 018	4 040	12 978
KEGG Annotation	11 969	3 170	8 799
KOG Annotation	11 847	2 508	9 339
NR Annotation	20 272	6 098	14 174
NT Annotation	39 740	19 229	20 511
Swissprot Annotation	16 701	38 74	12 827
All Annotated	40 987	20 256	20 731

A brighter red colour indicates a sample value close to 1, indicating a stronger correlation between two samples (Figure 1). The correlation between samples L1, L2, and L3 in this study was strong ($P > 0.6$). The correlation between B1, B2, and B3 was also good ($P > 0.6$). However, looking at the matrix, the correlation between maroon-feather quail samples (L1, L2, and L3) and white-feather quail samples (B1, B2 and B3) was relatively poor ($P < 0.6$). Therefore, the samples could be used for subsequent analysis.

**Figure 1** The sample correlation clustering chart of white-feather quail (B1, B2 and B3) and maroon-feather quail (L1, L2, and L3)

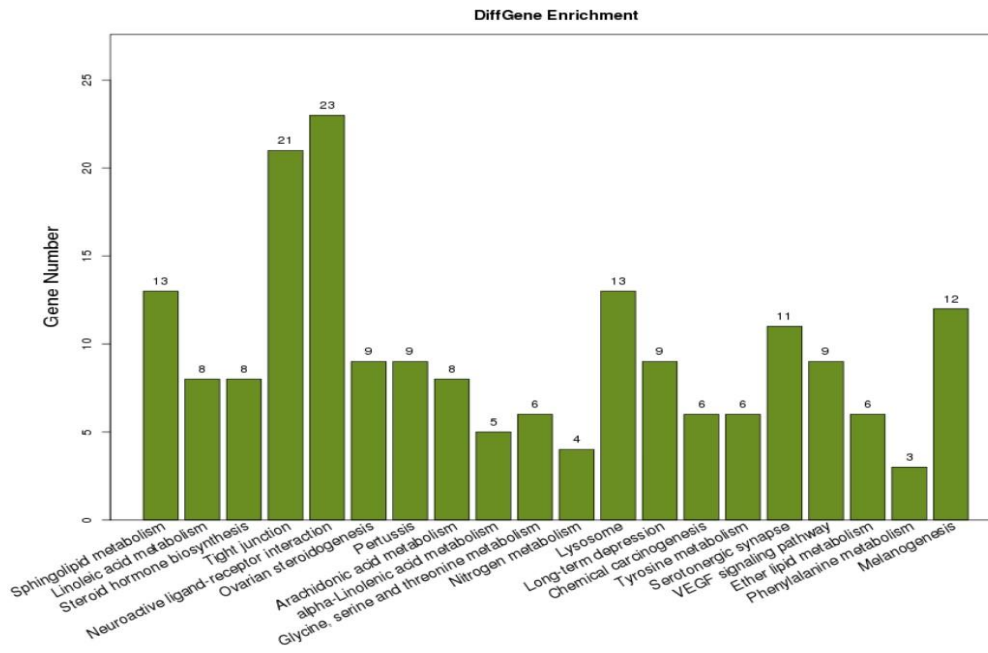


Figure 4 Differential gene KEGG pathway enrichment analysis diagram

The horizontal axis is the pathway name, and the vertical axis is the number of genes in the corresponding pathway.

Candidate genes were significantly different in the RNA-Seq database and played important roles in pigment synthesis, metabolism, and transport (Table 4).

Table 4 The statistics of genomic location, FDR, LogFC, and important function of candidate genes in RNA-Sequencing

GENE	Genomic location	FDR	LogFC	Function
Agouti signalling protein (ASIP)	NC_029535.1 (1422403-1441582)	0.000477	1.87979	promote feather whitening
DOPA decarboxylase (DDC)	NC_029517.1 (49924827-49991536)	4.10E-07	1.91715	reduce melanin synthesis
Homeobox D1 (HOXD1)	NC_029522.1 (14474309-14476761)	0.00347123	-1.14678	regulate pigment distribution
cathepsin D (CTSD)	NC_029520.1 (10422512-10435906)	6.28E-10	-2.508449	affects melanin metabolism
Methyl-CpG binding domain protein 2 (MBD2)	NW_015439872.1 (127509-154109)	8.84E-10	-1.944329	affects melanin metabolism
keratin 2 (KRT2)	NC_029544.1 (1127725-1132614)	0.002756	-2.34161	affects pigment transport
melatonin receptor 1 (MT1)	NC_029526.1 (554693-555815)	0.000542	-1.593388	promotes melanin synthesis

FDR (False Discovery Rate): Statistical significance level of difference analysis genes in RNA-seq. logFC: log₂ |FoldChange| value where logFC >1 indicates up-regulated, logFC <1 indicates down-regulated.

The reference genome of candidate genes: *Coturnix japonica* 2.1 (GCF_001577835.2)

The results of the qRT-PCR cq values of the seven candidate genes were calculated using 2^{-ΔΔct} (Figure 5). Of the candidate genes, *ASIP*, *DDC* were up-regulated and *HOXD1*, *KRT2*, *MT1*, *CTSD*, and *MBD2* were down-regulated in white-feather quails, which was consistent with the sequencing results of the transcriptome. The relative expression levels of white-and maroon-feather quails at 8 d, 12 d, and 14 d were the same as the result at 10 d. The expression levels of candidate genes were significantly different and constant at each stage in maroon- and white-feather quail embryos.

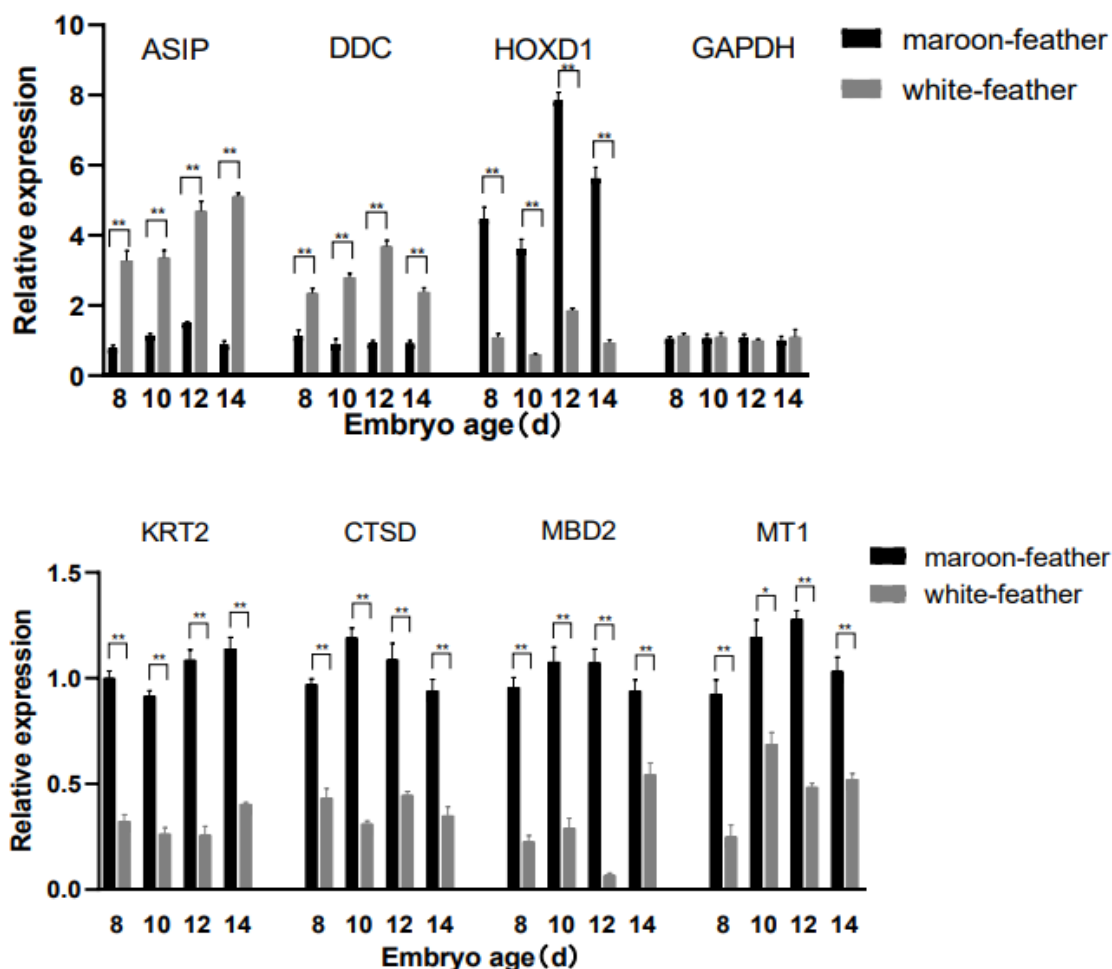


Figure 5 Relative expression of each candidate gene

The purpose of this study was to screen important DEGs and pathways associated with plumage colour using RNA-Seq and bioinformatics analysis in quail. After analysis of the transcriptomic data, the total number of DEGs in the maroon- and white-feather quail embryos of DEGs in the skin tissue was 2,514. Many DEGs were annotated in the GO and KEGG databases (Figure 3 and Figure 4). In GO annotations, keratinocyte differentiation, which was the most enriched in biological processes, was closely related to the transport of melanin. Moreover, the formation of melanosomes was dynamically related to the proliferation and differentiation of keratinocytes (Choi *et al.*, 2018). Highly enriched cellular components such as keratin filament, transcription factor complex, and intermediate filament are considered to be closely related to the transport of melanin in many studies (Shuster *et al.*, 1985; Stanic *et al.*, 2018). At present, it is known that at least three signal transduction pathways, adenylate cyclase, protein kinase C, and tyrosine kinase, exist in melanocytes and mediate the synthesis of melanin. Mediating these pathways often requires a variety of molecules. In terms of molecular function, many genes are highly correlated with melanin synthesis, and the enrichment is obvious, such as RNA polymerase II core promoter proximal region sequence specific DN binding and transcriptional activator activity, and RNA polymerase II core promoter proximal region (Ferguson *et al.*, 1997).

The completion of a physiological process in an organism requires the involvement and regulation of multiple genes. The plumage colour of the white-feather quails is a mutant trait. To elucidate its regulatory pathways, it was necessary to conduct KEGG signalling pathway analysis on DEGs. The enrichment count of neuroactive ligand-receptor interaction and tight junction pathways was 23 and 21, respectively. The neuroactive ligand-receptor interaction pathway may be related to macular disease, but its specific mechanism is not clear (Dhirachakulpanich *et al.*, 2020). The genes that relate tight junction pathways may play a regulatory role in the transfer of melanosomes from melanocytes to keratinocytes, and then affect the synthesis of melanin (Park *et al.*, 2020). The tyrosine metabolism and melanogenesis pathways, which are related to melanin synthesis, are enriched into six and 12 DEGs, respectively. The significant differences in tyrosinase (*TYR*), tyrosinase-related protein 1 (*TYRP1*), and

dopamine tautomerase (*DCT*), related to melanin synthesis, were marked in the two pathways, and *MC1R* appeared in the pathway with the highest enrichment. The tyrosine metabolism and melanogenesis pathways, which are related to melanin synthesis, were enriched into six and 12 differential genes, respectively, and the large differences in *TRY*, *TYRP1*, and *DCT*, related to melanin synthesis, were marked in the cycle; only melanocortin-1 receptor (*MC1R*) appeared in the pathway with the highest enrichment at the same time (Sun *et al.*, 2020). *TYRP1*, *TYR*, and *DCT* play a considerable role in the synthesis of melanin. If there are obvious changes in the tyrosine metabolism and melanoma pathways, they can affect the final synthesis of melanin to a great extent. The transcriptome expression of *TYRP1*, *TYR*, and *DCT* in white-feather quails was substantially lower than in maroon-feather quails, which was in line with the conclusion that the increase of *TYR* and other precursors for melanin synthesis will promote the increase in melanin synthesis. However, the increase of the relative expression of agouti signalling protein (*ASIP*) and *MC1R* may question this conclusion (Zhang *et al.*, 2017). The phenomenon that *ASIP* and *MC1R*, as melanin genes, increase their relative expression in albino quails, indicates that deeper research is needed to explore the mechanism causing maroon and white feathers. In summary, the current study suggests that the neuroactive ligand receptor interaction and tight junction pathways may be important pathways to further investigate the difference in feather colour in quail.

ASIP and DOPA decarboxylase (*DDC*) are involved in melanin synthesis and transport in different pathways. RNA-Seq and qRT-PCR results indicated that *ASIP* and *DDC* were significantly up-regulated in all stages of white-feather quail embryonic skin tissue (Table 4 and Figure 5). *ASIP* and *DDC* are involved in melanin synthesis and transport in different pathways. In black-bone chickens, the mRNA levels of *ASIP* are higher in black skin than in white skin (Yu *et al.*, 2019). The expression in duck embryos is higher in the abdomen than in the dorsum and is similar to the results of the present study (Baiz *et al.*, 2021). The antagonistic effect of *ASIP* on *MC1R* results in a black phenotype of hair follicle melanocytes (Chandramohan *et al.*, 2013), which is not observed in chicken skin but was marginally verified in the present study. The results of reduced total melanin in all mutant quail compared to wild-type quail (except brown quail; Minvielle *et al.*, 2009) were consistent with the results of the present study. The expression of *ASIP* may continue to increase in terms of the expression trend, although the expression level of *ASIP* reached its peak at 14 d in white-feather quail, whereas the expression level of *ASIP* showed a downward trend after 12 d in maroon-feather quail.

DDC is an important catalase for melanin synthesis in insects and its high expression would promote the formation of dopamine (Dion *et al.*, 2020). *DDC* is essential for the development of pigmentation in *Drosophila*, and the regulation of *DDC* and two other genes (*PALE* and *ABD-A*) may have evolved in concert, co-mapping a complex pattern of abdominal spots, indicating the presence of a regulatory effect on pigmentation (Grover *et al.*, 2018). In the current study, the significant differential expression of *DDC* in maroon- and white-feather quail in KEGG was mainly enriched in the tyrosine metabolism and serotonergic synapse pathways; the variation in its expression level was consistent with the results for both quail types. The increase in *DDC* may lead to a decrease in the tyrosine used for melanin synthesis which would promote albinism in quail. The expression level of *DDC* in white-feather quail decreased after reaching the highest level at 12 d, but the overall level was still higher than that in maroon-feather quail. It may promote the difference of feather colour in quail. The vertebrate central nervous system is more complex than that of insects and would be part of the reason that *DDC* affects pigment deposition. However, its specific mechanism needs further interrogation.

The remaining candidate genes affect feather colour traits in other ways (Table 4 and Figure 5). Homeobox D1 (*HOXD1*) plays a crucial role in head patterning in higher ruminants, and Allais-bonnet *et al.* (2021) demonstrated a blueprinted association between morphology and colour for this gene. The low expression of *HOXD1* in the current study resulted in the phenomenon of albinism in wild-type quail. The decrease of keratin 2 (*KRT2*) expression may promote the emergence of white feather traits. Fischer *et al.* (2014) found higher pigmentation in mice with high *KRT2* than it did in controls, which is similar to the findings of the current study. It has also been found that mutations in *KRT* in the dark skin of mice may impair intermediate filament assembly, leading to lysis of basal keratin-forming cells, secondary hyperkeratosis, and melanocytosis (Fitch *et al.*, 2003). The *KRT*'s mutations in their corresponding loci lead to increased tyrosine kinase activity *in vivo* and decreased levels of homeostatic receptors. The activation of cathepsin D (*CTSD*) was found to occur in the macular region in Rakoczy's study, which was similar to the results of the present study (Zhu *et al.*, 2013). Overexpression of *CTSD* has been researched in several human cancers, including melanoma (Rakoczy *et al.*, 1999), and it can degrade hormones, peptide precursors, polypeptides, and structural and functional proteins. In a series of activities, it may participate in and affect the metabolism of melanin, and finally promote the production of melanoma.

The expression of Methyl-CpG binding domain protein 2 (*MBD2*) is associated with transcriptional

activation/repression, chromatin structural regulation, pluripotency development, and differentiation (Menafrá *et al.*, 2014). Pan *et al.* (2014) showed that knockdown of *MBD2* causes more deposits to accumulate on the Bruch's membrane, which may reduce melanoma development by triggering choroidal endothelial activation and inflammatory responses, improving microcirculation, and reducing lipid deposition. This is similar to the results of the current study in which *MBD2* was less expressed in white-feather quail. The downregulation of melatonin receptor 1 (*MT1*) in the present study was similar to the findings of Shaverdashvili *et al.* (2014), who reported that a reduced expression of *MT1* facilitated the reduction of melanocyte metastasis.

Melatonin can stimulate the activity of tyrosinase and it would lead to increased melanin content in melatonin-treated cells. This is very similar to the relative expression of *MT1* in maroon- and white-feather quail in this study. *MT1* is a melatonin receptor that can be expressed in the skin and can induce pigment aggregation and skin whitening under certain conditions (Bertolesi *et al.*, 2020). Sugden *et al.* (1999) determined the phenomenon of melanin aggregation after its treatment. Many effects of *MT1* binding to melatonin, including the promotion of hair growth, were verified (Slominski *et al.*, 2012). The decrease in *MT1* expression may facilitate the formation of white feathers, which could provide a means of explaining the destination of melanin in maroon-feather quail.

Conclusions

In this study, seven DEGs related to the feather colour trait were screened using RNA-Seq, and the function, classification, and metabolic pathways of candidate genes were obtained: *ASIP* (promotes feather whitening), *DDC* (reduces melanin synthesis), *HOXD1* (regulates pigment distribution), *KRT2* (affects pigment transport), *MT1* (promotes melanin synthesis), *CTSD* (affects the metabolism of melanin), and *MBD2* (affects the metabolism of melanin). It was found that the neuroactive ligand receptor interaction and tight junction pathways could play an important role in the formation of quail feather colour. It was further verified that the melanin synthesis and tyrosine metabolism pathways played an important role in the formation of feather colour in quail. All the above DEGs may be utilized in future studies investigating the molecular regulation mechanism of genes related to feather colour traits in quail.

Acknowledgments

This study was supported by General Project of the Natural Science Foundation of Henan Province: Molecular Regulation of Black Feather Mutation and Feather Colour Selfing of Korean Quail (202300410153) and the Henan Science and Technology Research Project: Cultivation and Promotion of Egg Black Feather Quail Mating Lines (202102110088).

Authors' Contributions

Conceptualization: XHZ. Data curation: YQH, QKW, YWZ, ZWY, TW, LKH, and SWR. Analysis: YQH and XHZ. Funding acquisition: XHZ, YZP, and YXQ. Investigation: YQH, QKW, YWZ, ZWY, TW, LKH, SWR, and XHZ. Methodology: XHZ. Project administration: XHZ and YZP. Resources: QKW, YWZ, ZWY, and XHZ. Supervision: LKH and XHZ. Validation: YQH and XHZ. Writing: YQH.

Conflict of Interest Declaration

The authors declare that they have no conflicts of interest.

References

- Abolins-Abols, M., Kornobis, E., Ribeca, P., Wakamatsu, K., Peterson, M. P., Ketterson, E. D. & Milá, B, 2018. Differential gene regulation underlies variation in melanic plumage colouration in the dark-eyed junco (*Junco hyemalis*), *Mol. Ecol.* doi 10.1111/mec.14878
- Allais-Bonnet, A., Hintermann, A., Deloche, M. C., Cornette, R., Bardou, P., Naval-Sanchez, M., Pinton, A., Haruda, A., Grohs, C., Zakany, J., Bigi, D., Medugorac, I., Putelat, O., Greyvenstein, O., Hadfield, T., Jemaa, S. B., Bunevski, G., Menzi, F., Hirter, N., Paris, J. M., Hedges, J., Palhiere, I., Rupp, R., Lenstra, J. A., Gidney, L., Lesur, J., Schafberg, R., Stache, M., Wandhammer, M. D., Arbogast, R. M., Guintard, C., Blin, A., Boukadiri, A., Rivière, J., Esquerré, D., Donnadiou, C., Danchin-Burge, C., Reich, C. M., Riley, D. G., Marle-Koster, E. V., Cockett, N., Hayes, B. J., Drögemüller, C., Kijas, J., Pailhoux, E., Tossier-Klopp, G., Duboule, D. & Capitan, A., 2021. Analysis of polycerate mutants reveals the evolutionary co-option of *HOXD1* for horn patterning in Bovidae. *Mol Biol Evol.* 38, 2260-72. doi 10.1093/molbev/msab021
- Baiz, M. D., Wood, A. W., Brelsford, A., Lovette, I. J. & Toews, D. P. L., 2021. Pigmentation genes show evidence of repeated divergence and multiple bouts of introgression in Setophaga Warblers. *Curr Biol.* 31, 643-49.e3. doi 10.1016/j.cub.2020.10.094
- Bertolesi, G. E., Atkinson-Leadbeater, K., Mackey, E. M., Song, Y. N., Heyne, B. & McFarlane, S., 2020. The regulation of skin pigmentation in response to environmental light by pineal Type II opsins and skin melanophore melatonin receptors. *J Photochem Photobiol B.* 212, 112024. doi 10.1016/j.jphotobiol.2020.112024

- Chandramohan, B., Renieri, C., La Manna, V. & La Terza, A., 2013. The alpaca agouti gene: Genomic locus, transcripts, and causative mutations of eumelanic and pheomelanic coat colour. *Gene*. 521, 303-10. doi 10.1016/j.gene.2013.03.060
- Choi, H. I., Sohn, K. C., Hong, D. K., Lee, Y., Kim, C. D., Yoon, T. J., Park, J. W., Jung, S., Lee, J. H. & Lee, Y. H., 2014. Melanosome uptake is associated with the proliferation and differentiation of keratinocytes. *Arch Dermatol Res*. 306, 59-66. doi 10.1007/s00403-013-1422-x
- Dhirachaikulpanich, D., Li, X., Porter, L. F. & Paraoan, L., 2020. Integrated microarray and RNAseq Transcriptomic analysis of retinal pigment epithelium/choroid in age-related macular degeneration. *Front Cell Dev Biol*. 8. doi 10.3389/fcell.2020.00808
- Dion, W. A., Shittu, M. O., Steenwinkel, T. E., Raja, K. K. B., Kokate, P. P. & Werner, T., 2020. The modular expression patterns of three pigmentation genes prefigure unique abdominal morphologies seen among three *Drosophila* species. *Gene Expr Patterns*. 38, 119132. doi 10.1016/j.gep.2020.119132
- Ferguson, C. A. & Kidson, S. H., 1997. The regulation of tyrosinase gene transcription. *Pigment Cell Research*. 10, 127-38. doi 10.1111/j.1600-0749.1997.tb00474.x
- Fischer, H., Langbein, L., Reichelt, J., Praetzel-Wunder, S., Buchberger, M., Ghannadan, M., Tschachler, E. & Eckhart, L., 2014. Loss of keratin K2 expression causes aberrant aggregation of K10, hyperkeratosis, and inflammation. *J Invest Dermatol*. 134, 2579-88. doi 10.1038/jid.2014.197
- Fitch, K. R., McGowan, K. A., van Raamsdonk, C. D., Fuchs, H., Lee, D., Puech, A., Hérault, Y., Threadgill, D. W., Hrabé de Angelis, M. & Barsh, G. S., 2003. Genetics of dark skin in mice. *Genes Dev*. 17, 214-28. doi 10.1101/gad.1023703
- Grover, S., Williams, M. E., Kaiser, R., Hughes, J. T., Gresham, L., Rebeiz, M. & Williams, T. M., 2018. Augmentation of a wound response element accompanies the origin of a HOX-regulated *Drosophila* abdominal pigmentation trait. *Dev Biol*. 441, 159-75. doi 10.1016/j.ydbio.2018.07.001
- Inaba, M. & Chuong, C. M., 2020. Avian pigment pattern formation: Developmental control of macro- (across the body) and micro- (within a feather) level of pigment patterns. *Front Cell Dev Biol*. 8, 8. doi 10.3389/fcell.2020.00620
- Javůrková, V. G., Enbody, E. D., Kreisinger, J., Chmel, K., Mrázek, J. & Karubian, J., 2019. Plumage iridescence is associated with distinct feather microbiota in a tropical passerine. *Sci Rep*. 9, 12921. doi 10.1038/s41598-019-49220-y
- Livak K. J., Schmittgen, T. D., 2001. Analysis of relative gene expression data using real-time quantitative PCR and the 2⁻(Delta Delta C(T)) method. *Methods*, 25(4), 402-8. doi: 10.1006/meth.2001.1262.
- Menafrá, R. & Stunnenberg, H. G., 2014. MBD2 and MBD3: Elusive functions and mechanisms. *Front Genet*. 5, 428. doi 10.3389/fgene.2014.00428
- Minvielle, F., Cecchi, T., Passamonti, P., Gourichon, D. & Renieri, C., 2009. Plumage colour mutations and melanins in the feathers of the Japanese quail: A first comparison. *Anim Genet*. 40, 971-4. doi 10.1111/j.1365-2052.2009.01929.x
- Ng, C. S. & Li, W. H., 2018. Genetic and molecular basis of feather diversity in birds. *Genome Biol Evol*. 10, 2572-86. doi 10.1093/gbe/evy180
- Niwa, T., Shibusawa, M., Matsuda, Y., Terashima, A., Nakamura, A. & Shiojiri, N., 2003. The Bh (black at hatch) gene that causes abnormal feather pigmentation maps to chromosome 1 of the Japanese quail. *Pigment Cell Res*. 16, 656-61. doi 10.1046/j.1600-0749.2003.00096.x
- Pan, J. R., Wang, C., Yu, Q. L., Zhang, S., Li, B. & Hu, J., 2014. Effect of Methyl-CpG binding domain protein 2 (MBD2) on AMD-like lesions in ApoE-deficient mice. *J Huazhong Univ Sci Technolog Med Sci*. 34, 408-14. Doi 10.1007/s11596-014-1292-2
- Park, M., Woo, S. Y., Cho, K. A., Cho, M. S. & Lee, K. H., 2020. PD-L1 produced by HaCaT cells under polyinosinic-polycytidylic acid stimulation inhibits melanin production by B16F10 cells. *Plos One*. 15. doi 10.1371/journal.pone.0233448
- Rakoczy, P. E., Sarks, S. H., Daw, N. & Constable, I. J., 1999. Distribution of cathepsin D in human eyes with or without age-related maculopathy. *Exp Eye Res*. 69, 367-74. Doi 10.1006/exer.1999.0700
- Shaverdashvili, K., Wong, P., Ma, J., Zhang, K., Osman, I. & Bedogni, B., 2014. MT1-MMP modulates melanoma cell dissemination and metastasis through activation of MMP2 and RAC1. *Pigment Cell Melanoma Res*. 27, 287-96. doi 10.1111/pcmr.12201
- Shuster, S., Huszar, M. & Geiger, B., 1985. Immunofluorescent localization of intermediate filament subunits for the differential diagnosis of malignant melanoma. *Am. J. Dermatopathol*. 7 Suppl, 79-86.
- Slominski, R. M., Reiter, R. J., Schlabritz-Loutsevitch, N., Ostrom, R. S. & Slominski, A. T., 2012. Melatonin membrane receptors in peripheral tissues: Distribution and functions. *Mol Cell Endocrinol*. 351, 152-66. doi 10.1016/j.mce.2012.01.004
- Stanic, V., Maia, F. C. B., Freitas, R. D., Montoro, F. E. & Evans-Lutterodt, K., 2018. The chemical fingerprint of hair melanosomes by infrared nano-spectroscopy. *Nanoscale*. 10, 14245-53. doi 10.1039/c8nr03146k
- Sugden, D., Yeh, L. K. & Teh, M. T., 1999. Design of subtype selective melatonin receptor agonists and antagonists. *Reprod Nutr Dev*. 39, 335-44. doi 10.1051/rnd:19990306
- Sun, L., Zhou, T., Wan, Q. H. & Fang, S. G., 2020. Transcriptome comparison reveals key components of nuptial plumage colouration in Crested Ibis. *Biomolecules*. 10. doi 10.3390/biom10060905
- Tsudzuki, M., Kusano, S., Wakasugi, N., Morioka, H. & Esaki, K., 1992. Dotted white, a plumage colour mutant in Japanese quail (*Coturnix coturnix japonica*). *Jikken Dobutsu*. 41, 25-31.
- Wang, Q., Zhang, X., Pang, Y., Qi, Y., Lei, Y., Bai, J., Hu, Y., Zhao, Y., Yuan, Z. & Wang, T., 2022. Screening of genes related to auto-sexing on feather colour based on RNA-Seq technology. *Acta Agriculturae*

- Zhejiangensis. 34(03), 498-506. doi 10.3969/j.issn.1004-1524.2022.03.10
- Yu, S., Wang, G. & Liao, J., 2019. Association of a novel SNP in the ASIP gene with skin colour in black-bone chicken. *Anim Genet.* 50, 283-86. doi 10.1111/age.12768
- Zhang, Y. Q., Liu, J. H., Peng, L. Y., Ren, L., Zhang, H. Q., Zou, L. J., Liu, W. B. & Xiao, Y. M., 2017. Comparative transcriptome analysis of molecular mechanism underlying gray-to-red body colour formation in red crucian carp (*Carassius auratus*, red var.). *Fish Physiol. Biochem.* 43, 1387-98. doi 10.1007/s10695-017-0379-7
- Zhu, L., Wada, M., Usagawa, Y., Yasukochi, Y., Yokoyama, A., Wada, N., Sakamoto, M., Maekawa, T., Miyazaki, R., Yonenaga, E., Kiyomatsu, M., Murata, M. & Furue, M., 2013. Overexpression of cathepsin D in malignant melanoma. *Fukuoka Igaku Zasshi.* 104, 370-5.